



Preparation and Characterization of Polyvinyl Alcohol/Activated Carbon (PVA/AC) Composite and Its Use in the Adsorption of 4-Nitrophenol (4-NP)

Hatice KARAER YAĞMUR^{1,*}

¹Dicle University, Faculty of Science, Department of Chemistry, Diyarbakır, Turkey
profhatice23@hotmail.com, ORCID: 0000-0002-3728-1825

Received: 02.10.2019

Accepted: 26.03.2020

Published: 25.06.2020

Abstract

In this study, polyvinyl alcohol-activated carbon (PVA/AC) composite was synthesized and characterized by SEM, FTIR, DLS and TGA-DSC measurement. The zero point charge for the PVA/AC was determined as approximately 3 pH. The efficiency of PVA/AC as a cheap adsorbent for removal of 4-nitrophenol (4-NP) from aqueous solution was researched at 298, 318 and 328 K. For this purpose, Freundlich and Langmuir isotherm models were used. According to the results, adsorption of 4-NP onto composite best fitted to Freundlich model. The pseudo-first-order, pseudo-second-order and intraparticle diffusion models were utilized to study the adsorption kinetics. The experimental consequences fitted with the pseudo-first-order model. According to Arrhenius equation, E_a was calculated as 14.13 kJmol^{-1} . Thermodynamic parameters were also calculated, which revealed that the adsorption process is endothermic, not spontaneous.

Keywords: Adsorption; Activated carbon; Polyvinyl alcohol; 4-nitrophenol (4-NP); Zero point charge.

Polivinil Alkol/Aktif Karbon (PVA/AC) Kompozitinin Hazırlanması ve Karakterizasyonu ve 4-Nitrofenol (4-NP) Adsorpsiyonunda Kullanımı



Öz

Bu çalışmada polivinil alkol/aktif karbon (PVA/AC) kompoziti sentezlendi ve SEM, FTIR, DLS ve TGA-DSC ölçümleriyle karakterize edildi. PVA/AC için sıfır noktası yükü yaklaşık 3 pH olarak belirlenmiştir. Sulu çözeltiden 4-nitrofenolün (4-NP) uzaklaştırılması için ucuz bir adsorban olarak PVA / AC'nin etkinliği 298, 318 ve 328 K'de araştırıldı. Bu amaçla Freundlich ve Langmuir izoterm modelleri kullanıldı. Sonuçlara göre, 4-NP'nin kompozit üzerine adsorpsiyonunda Freundlich model en uygundu. Adsorpsiyon kinetiklerini incelemek için psödo birinci derece, psödo ikinci derece ve partikül içi difüzyon modelleri kullanıldı. Deneysel sonuçlar psödo birinci derece modeline uydu. Arrhenius denklemine göre E_a , 14.13 kJmol⁻¹ olarak hesaplandı. Termodinamik parametreler hesaplandı, adsorpsiyon sürecinin endotermik olduğu kendiliğinden olmadığı belirlendi.

Anahtar Kelimeler: Adsorpsiyon; Aktif karbon; Polivinil alkol; 4-nitrofenol (4-NP); Sıfır nokta yükü.

1. Introduction

Activated charcoals (ACs) are known homogeneous materials having high surface area and microporous structure. Moreover, they are widely used in industrial applications as adsorbent and catalyst. The features of AC adsorption depend primarily upon size of particle, porosity, ash contents, carbonization degree and activation process [1]. Moreover, they are efficiently used both in purification of drinking water and different industrial applications and in hemoperfusion and based on hemofiltration therapies [2]. Polyvinyl alcohol (PVA) is a water-soluble synthetic polymer and is known as a cheap polymer and not poisonous [3]. Between artificial polymers, PVA has received amazing interest owing to its convenient physicochemical and viscoelastic features and is widely utilized for several biomedical functions for wound dressing and tissue engineering since it is a biodegradable as well as biocompatible artificial polymer [4]. Phenolic compounds have been widely utilized in the production of chemicals such as explosives, dyes, pesticides, solvents and can stay in aqueous media for a long time. Phenols have been encountered in both wastewater and in whole natural aquatic systems, and have toxic features even at low concentrations. 4-nitrophenol (4-NP) is one of the phenol derivatives which is toxic. 4-NP has a hydroxyl group at the opposite side of a nitro group on the benzene ring and is generally found in wastewater especially with pesticides, herbicides and petrochemicals [5]. Elimination of the phenolic compounds from water is an interesting field due to their high stability and solubility, and the development of environmentally friendly techniques for elimination of phenolic compounds from polluted water is still an important significant topic. Currently, several methods,

such as separation of membrane, adsorption and exchange of ion have been utilized for the elimination of phenolic compounds from industrial effluents. Adsorption method is one of the efficient and preferred processes due to its simplicity and high effectiveness [6]. There are many studies in the literature on activated carbon. However, the studies on polyvinyl alcohol/activated carbon and 4-nitrophenol (4-NP) are limited.

In this study, a new polymer-based composite was prepared from PVA and AC. The composite was characterized by FTIR, DLS, SEM-EDX, TGA-DSC and Zeta sizer. Furthermore, the point of zero charge of PVA/AC composite was determined. Then, PVA/AC composite was used as an adsorbent for the removal of 4-nitrophenol (4-NP) from aqueous solution. Finally, the adsorption of 4-NP by the PVA/AC composite from aqueous solution was studied both thermodynamically and kinetically.

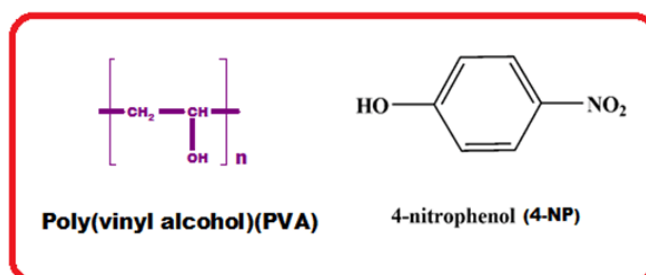
2. Materials and Methods

2.1. Materials

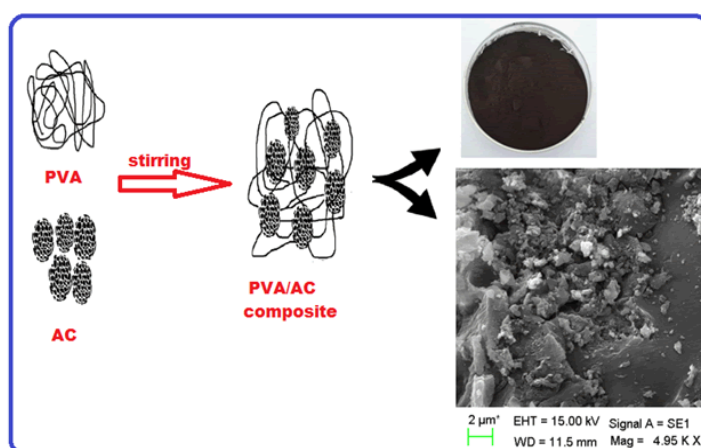
PVA (Poly(vinyl alcohol) was supplied from Sigma–Aldrich (average molecular weight (M_w): 30,000-70,000 g mol^{-1} and 90% hydrolyzed). AC (Activated charcoal, black powder, 100-400 mesh) and 4-Nitrophenol (4-NP) were bought from Sigma and Sigma–Aldrich (M_w : 139.11 g mol^{-1}) respectively.

2.2. Preparation of PVA/AC composite

The composite was synthesized according to a reported procedure [2, 7]. A solution of PVA was synthesized from PVA (5 g) and distilled water (100 mL) at 90 °C with vigorous stirring. Then, an aqueous solution of PVA and 10 mL sulfuric acid was mechanically stirred in a 500 mL beaker, and temperature of the mixture was diminished to 60 °C. Subsequently, AC (2.5 g) was added and stirred. The mixture was cooled to room temperature and kept in an ice bath for 30 min. 5 mL of 25% glutaraldehyde solution was added to the cooled solution and the mixture was stirred by a magnetic stirrer for about 3h. PVA/AC composite was acquired after washing with distilled water. It was dried in an oven at about 80 °C. Scheme 2 shows the PVA/AC preparation (Scheme 2).



Scheme 1: The chemical structure of materials



Scheme 2: Schematic representation of PVA/AC composite preparation

2.3. Characterization

The chemical structure of the composite was elucidated by using FTIR spectroscopy (A Perkin Elmer spectrometer-ATR sampling accessory between the wavelengths of 4000–450 cm^{-1}). TGA–DTA analysis was carried out between 20 and 1000 °C (Perkin Elmer, in N_2 , rate 10 °C min^{-1}). DSC analysis of the composite was performed between 25 and 450 °C (Perkin Elmer Pyris sapphire, in N_2 , rate 10 °C min^{-1}). Surface structure of the composite was identified by using of SEM (scanning electron microscope, JEOL, JSM-7100 model). The conductivity measurements were performed by Keithley Electrometer (Keithley 2400, Ohio, USA). The pellet was pressed on hydraulic press at 1687 kg/cm^2 . Iodine doping was performed by exposing the pellet to iodine steam at 25 °C in a desiccator. Particle dimension of the PVA/AC was detected by using the DLS (dynamic light scattering) method. Zeta potential measurement of the PVA/AC was performed using a ZetaSizer Nano-ZS (Malvern Nano ZS90).

2.4. Determination of the point of zero charge (pH_{zpc})

The point of zero charge was determined by a reported procedure [8, 9]. The procedure can be described as follows: to a series of 50 mL conical flasks, 30 mL of 0.1M NaCl solution was added. pH values of the initial NaCl solutions (initial pH) were adjusted in the range of 2 to 12 of using 0.1 M HCl / NaOH solutions. After a constant value of initial pH had been reached, 0.015 g of PVA/AC composite was added into each conical flask and capped them immediately. These samples were shaken for 48 h, after which pH was measured for each sample (pH_f). The pH variation ($\Delta\text{pH} = \text{pH}_f - \text{pH}_i$) was plotted against the pH_i, and the point of intersection of the resulting curve at which $\Delta\text{pH} = 0$ was the pH_{zpc} value.

2.5. Adsorption kinetics and isotherms

The sorption studies were performed on the composite by use of 4-NP (Scheme 1) and can be classified as three parts: (a) effect of temperature (b) defining of a kinetic model and isotherm model (c) thermodynamic studies. Kinetic studies were performed agitating 100 ml of solution of a constant 4-NP concentration with 0.1 g of the composite at the shaking rate 120 rpm, 298, 313 and 328 K, natural pH. Adsorption equilibrium studies were performed by 0.05 g of composite with 100 mL of 4-NP solution of in the range of 50 to 500 mgL⁻¹ concentrations at 298, 313 and 328 K (S.R:120 rpm for 4h). The equilibrium phenol concentration was measured via a UV-visible spectroscopy (λ_{max} :348 nm for 4-NP, Cary 100 Bio UV-visible spectrophotometer). The capacity of adsorption (q_e , mg g⁻¹) may be computed by the following equations:

$$q_e = (\text{Co} - \text{Ce}) V/m \quad (1)$$

V (L), Co (mgL⁻¹), m (g) and Ce (mg L⁻¹) are the volume of the solution, initial concentration, the adsorbent mass and equilibrium concentration of phenol in the solution, respectively.

3. Results and Discussion

3.1. FTIR

FTIR spectra of PVA and PVA/AC were shown in Fig. 1. The PVA has -CH₂, -CH and -OH groups with C-C backbone and is known as a polar polymer. The formation of intermolecular and free bonded hydroxyl groups of AC and PVA were observed at 3317 cm⁻¹. The aliphatic stretching peak of C-H was observed at 2971 cm⁻¹ and 2901 cm⁻¹. The peaks at 1702 cm⁻¹ and 1667 cm⁻¹ are due to C=O and C-O stretching, respectively. The peaks at around 1596 cm⁻¹ and 1409 cm⁻¹ are corresponding to C=C vibrations and the C-H aliphatic bending, respectively. The

peak at 1080 cm^{-1} (PVA) was defined C-O stretching peak in alcohols. The broadening of C-O peak (1080 cm^{-1}) occurred with the existence of a new peak at 1049 cm^{-1} in the composite is attributed to the interfacial covalent reaction between AC and PVA. The peak at 829 cm^{-1} (PVA) for C-H bending in the PVA/AC sample shifted to 809 cm^{-1} with AC addition [4].

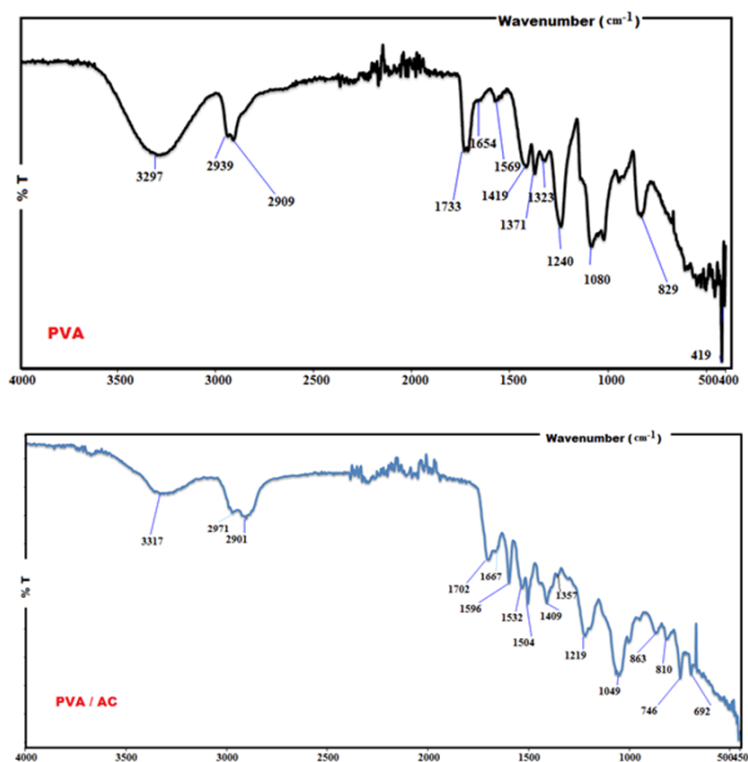


Figure 1: FTIR spectra of the PVA and PVA/AC

3.2. SEM-EDX analysis

The surface morphology of PVA/AC composite was determined by using SEM (Fig. 2). EDX has been defined as the elements on the composite surface. Fig. 2, shows the SEM images of the composite. One can easily see in the Fig. 2 that the surface of the composite is amorphous and not regular, which shows a relatively high surface area. EDX analysis shows that the composite is composed commonly of carbon (Fig. 2(B)). The peaks related to oxygen are low and there were no other different atoms (N, P, S.) present in the composite.

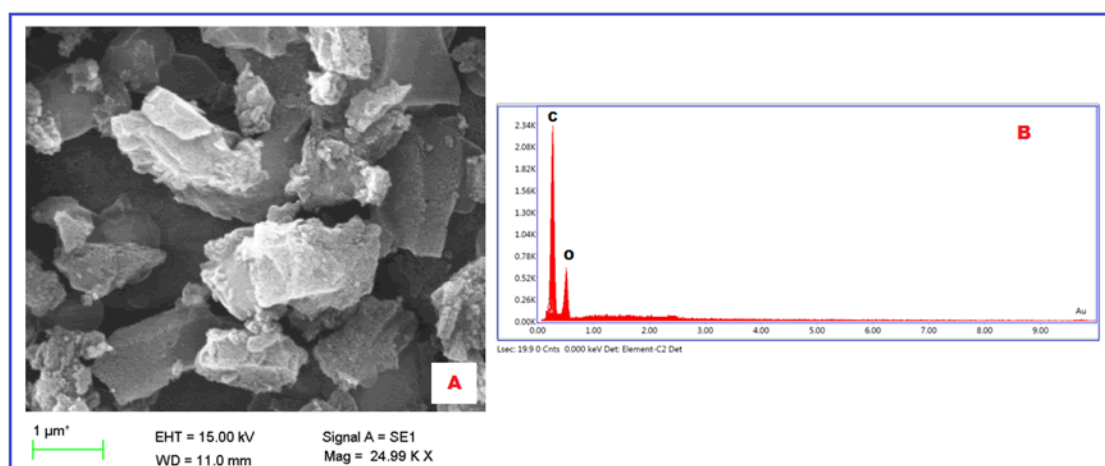


Figure 2: SEM image of composite (A) and EDX spectra of composite (B)

3.3. Dynamic light scattering (DLS)

633 nm diode laser was used in the instrument. The PVA/AC composite was diluted by using of pure water before measurement. The D-values (D10, D50 and D90) were usually used for describing particle size distributions. D10, D50 and D90 are the intercepts for 10%, 50% and 90% of the cumulative mass [10]. Size distribution of the PVA/AC particles was found as $< 14.3 \mu\text{m} < 299 \mu\text{m} < 1170 \mu\text{m}$ for D10, D50 and D90% cumulative mass, respectively. For example, if the D50 is 299 μm, for PVA/AC particles, this means that 50% of the PVA/AC particles has a size of 299 μm or smaller. An additional parameter to show the width of the size distribution is the span. The span of a volume-based size distribution is determined as $\text{Span} = (D90 - D10)/D50$ and gives an indication of how far the 10 percent and 90 percent points are apart, normalized with the midpoint [10]. The value of span PVA/AC was calculated as 3.86.

3.4. Thermal studies

TGA, DTA, DTG and DSC are defined as Thermogravimetric analysis, Differential Thermal Analysis, Differential Thermogravimetry and Differential Scanning Calorimetry respectively. TGA, DTG, DTA and DSC curves of the composite were given in Fig. 3. Based on TGA analysis, Tonset (the initial degradation temperatures) of the PVA/AC composite was defined as 170 °C. The values of temperature of T₂₀ (20%, weight losses) and T₅₀ (50%, weight losses) were defined as 233 and 446 °C, respectively. Tmax was defined from the DTG curves as 194 and 433°C. The endothermic and exothermic peaks were not observed in DTA curve of the composite. The glass transition temperature (T_g) and the change in the specific heat (ΔC_p) during the glass transition of the composite were computed from its DSC curve as 147 °C and 0.106 J/g °C.

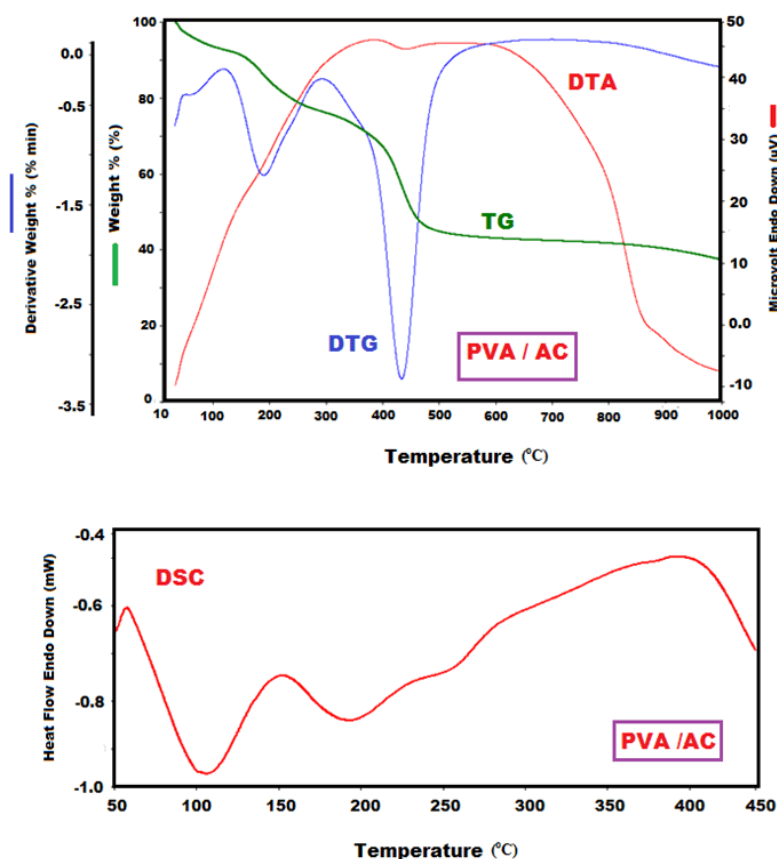


Figure 3: TGA and DSC analysis curves of the PVA/AC

3.5. Conductivity of the composite

The composite pellet was doped with iodine vapors at 25 °C in desiccators for 24 h. It was observed that the conductivity of the PVA/AC increased slightly but then tended to level-off. The conductivities of doped and undoped pressed PVA/AC pellets were determined as $2.44 \times 10^{-5} \text{ S cm}^{-1}$ and $2.09 \times 10^{-4} \text{ S cm}^{-1}$, respectively.

3.6. Point of zero charge

The sorbent surface to charge positively or negatively depends on concentration of protons in the solution. The pH_{pzc} results of the experiments were determined with the PVA/AC composite, where the pH ranged from 2 to 12. Fig. 4 shows that the pH_{pzc} of the PVA/AC was approximately 3. In other words, at this pH, the PVA/AC surface has zero charge [9]. Therefore, when solution pH increases above pH_{pzc}, the surface of PVA/AC is negatively charged, when it decreases below the pH_{pzc} value the surface of PVA/AC is positively charged because of protonation [11, 12].

4-NP is a weak acid (pKa value of 7.15). If initial pH of the solution is in acidic range, particularly less than 3, the most of 4-NP molecules remain in molecular form and at the same time the PVA/AC surface possesses positive charge due to pH_{pzc} (i.e. 3). If initial pH of the solution is in alkaline range, the dissociation of 4-NP into 4-NP anions takes place and at the same time the PVA/AC surface possesses negative charge (because pH > pH_{pzc}). In this state electrostatic repulsion dominates between the adsorbate and adsorbent surface, resulting in a considerable decrease in percentage removal of 4-NP in alkaline range. At pH of 3.0 the net charge on the PVA/AC surface was zero, hence, there was no electrostatic repulsion and hence the removal of 4-NP is more than that in alkaline range [13]. Fig. 5 shows the zeta potential curves of PVA/AC in three replicates. Zeta potential value of PVA/AC was -17.8 mV. Therefore, the PVA/AC composite has a negative surface charge and may be moved towards a positively polarized electrode under an electric field [14]. Nanoparticles with zeta potential greater than +30mV or less than -30mV are considered strongly cationic and strongly anionic respectively [15]. Paralikar [16] reported that negative zeta potential value of the particles might be owing to adsorption of OH⁻ ions on adsorbent. OH⁻ ion helps in preventing the aggregation.

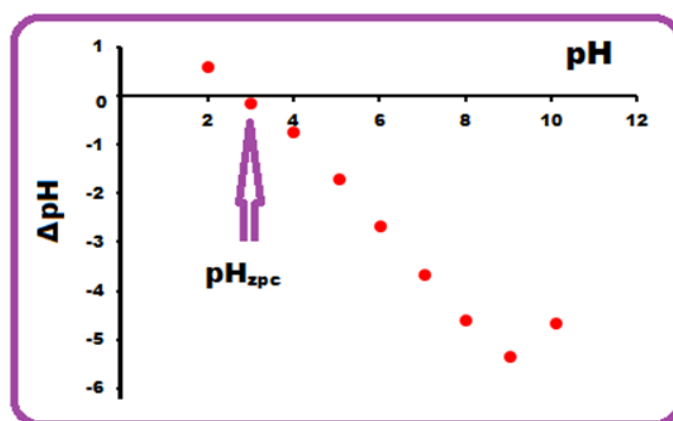


Figure 4: Zero point charge of PVA/AC at 298 K

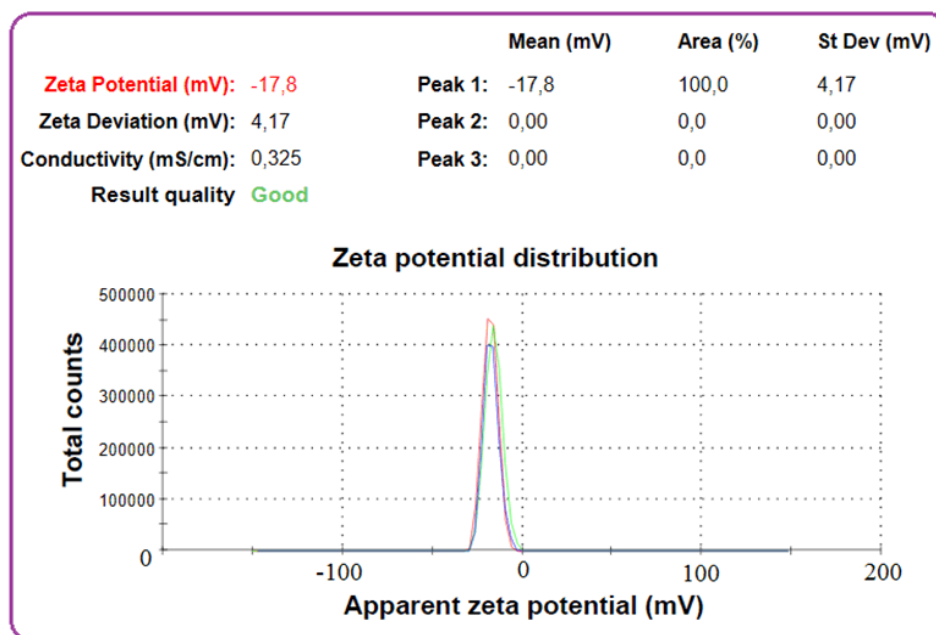


Figure 5: Zeta potential curves obtained for water suspensions of PVA/AC

3.7. Kinetic study

3.7.1. Effect of temperature

The effect of contact time on the sorption of 4-NP by the PVA/AC was researched for 200 min by using initial 4-NP concentration of 100 mg/L. Fig. 6 shows the quantity of adsorbed 4-NP (q_e , mg g⁻¹) at 298, 313 and 328 K. The values of q_e (mg g⁻¹) increased from 298 to 313 K, indicating that the adsorption of 4-NP on the PVA/AC composite is endothermic. Three different kinetic models (Lagergren(PFO), Ho-Mckay(PSO) and Weber-Morris) were used to understand the adsorption process:

Pseudo-first order (PFO)

$$\log (q_e - q_t) = \log q_e - k_1 t / 2.303 \quad (2)$$

Pseudo-second order (PSO)

$$t / q_t = 1 / k_2 q_e^2 + t / q_e \quad (3)$$

Intra particle diffusion(Weber-Morris)

$$q_t = k_{id} t^{1/2} + C \quad (4)$$

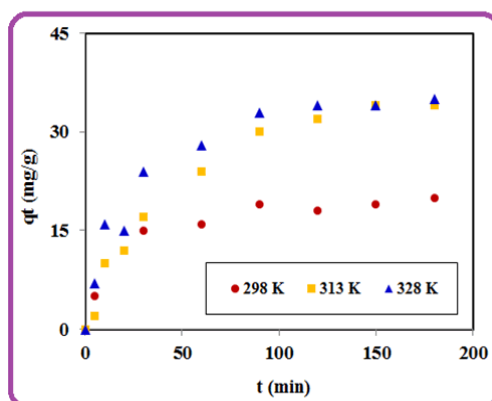


Figure 6: Adsorption kinetic of 4-NP on the composite at 298, 313, 328 K

q_e (mg g^{-1}) and q_t (mg g^{-1}) are the quantity of adsorbed at equilibrium and at any contact time of adsorption t (min), respectively; PFO, PSO and intraparticle diffusion rate constants were defined as k_1 (min^{-1}), k_2 ($\text{g mg}^{-1} \text{min}^{-1}$), and k_{id} ($\text{mg g}^{-1} \text{min}^{-1/2}$) respectively. Based on Eqn.(2), the plot of $\log(q_e - q_t)$ versus t , and based on Eqn.(3) the plot of t/q_t versus t and based on Eqn. (4) the plot of q_t versus $t^{1/2}$ should each give a straight line for the respective model to be applicable [17]. The rate constants, q_e and correlation coefficient values (R^2) were shown in Table 1. Table 1 and Fig. 7 show the kinetic models of sorption for 4-NP. Based on the results (Table 1), PFO model has higher values of correlation coefficients (R^2) compared to PSO model. Moreover, the computed q_e values agreed with the experimental q_e data in the case of the PFO model [18]. Feyzi et al. used raw and modified activated carbon from walnut and pistachio shell in order to remove Dimethyl sulfide from model fuel. Results showed that adsorption kinetic could be determined by pseudo-first order kinetic model [19]. Nam et al. synthesized active carbon from peanut shell with KOH activation for the adsorption of H_2S . According to their results, adsorption kinetic was determined as the pseudo-first order model owing to its higher R^2 and smaller difference between $q_{e,\text{exp}}$ and $q_{e,\text{calc}}$ as compared to the pseudo-second order model [20]. Moreover, the best-fitted model can be determined using the normalized standard deviation (Δq_e (%)) and average relative error (ARE) [21, 22]. The equations of the functions are given as follows:

$$\Delta q_e(\%) = 100 \times \sqrt{\frac{1}{n-1} \sum_{i=1}^n \left[\frac{q_{t,\text{meas}} - q_{t,\text{cal}}}{q_{t,\text{meas}}} \right]^2} \quad (5)$$

$$ARE = \frac{100}{n} \sum_{i=1}^n \left[\frac{q_{t,\text{meas}} - q_{t,\text{cal}}}{q_{t,\text{meas}}} \right] \quad (6)$$

$q_{t,\text{meas}}$ (mg/g), $q_{t,\text{cal}}$ (mg/g) and n are the experimental and calculated equilibrium adsorption capacity and value the number of data points respectively. The values of Δq_e and ARE were

shown in Table 1. Low ARE and Δq_e (%) values indicate the accurate fitting of the model [21, 23]. According to our experimental results (Table 1), it may be seen that the pseudo-first order (PFO) model seems to be suitable for modelling the adsorption of 4-NP on PVA/AC.

Table 1: Kinetic data

T (K)	Pseudo First Order (PFO)						Pseudo Second Order (PSO)				Intra-Particle Diffusion Model		
	$q_{e,exp}$ (mg g ⁻¹)	$q_{e,calc}$ (mg g ⁻¹)	$k_1 \times 10^3$ (min ⁻¹)	R ²	Δq_e (%)	ARE	$q_{e,calc}$ (mg g ⁻¹)	$k_2 \times 10^3$ (g mg ⁻¹ min ⁻¹)	R ²	Δq_e (%)	ARE	k_{id} (mgg ⁻¹ min ^{-1/2})	R ²
298	21	19.17	17.50	0.8647	3.1	0.97	20.58	4.36	0.9928	0.005	0.22	1.36	0.8639
313	35	34.40	23.26	0.9932	0.61	0.19	43.86	0.48	0.8680	9.0	2.81	2.94	0.8003
328	35	32.64	29.48	0.9857	2.4	0.75	38.02	1.57	0.9685	3.0	0.97	2.63	0.9131

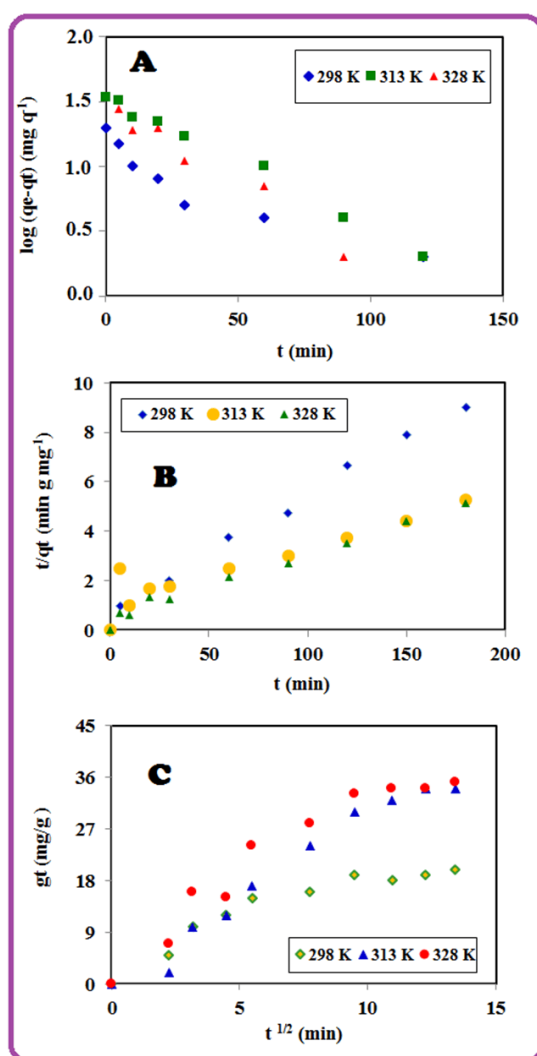


Figure 7: Fitting of Lagergren (PFO) (A), Ho-Mckay (PSO) (B) and intra-particle diffusion (Weber-Morris) (C) kinetic models

3.7.2. Activation parameters

The adsorption type was defined by using the PFO rate constants(k_1) at 298, 313, 328 K and the Arrhenius eqn. (7),

$$\log k_1 = \log A - E_a/2.303RT \quad (7)$$

where E_a , k_1 , A , R and T are the activation energy (Jmol^{-1}), the PFO rate constant(min^{-1}), the Arrhenius factor ($\text{gmol}^{-1}\text{min}^{-1}$), the gas constant ($8.314 \text{ J K}^{-1} \text{ mol}^{-1}$) and the temperature (K) respectively.

The slope of the plot of $\ln k_1$ versus $1/T$ was used to evaluate E_a (Figure not given). Physical adsorption has low activation energies (between $5\text{--}40 \text{ kJ mol}^{-1}$), while chemical chemisorption has higher ones ($40\text{--}800 \text{ kJ mol}^{-1}$) [24, 25]. Based on the results, the adsorption of 4-NP on the composite is physisorption because of $E_a=14.13 \text{ kJmol}^{-1}$.

3.8. Adsorption isotherm parameters

The adsorption isotherms studies for evaluating adsorption process are essential to attain some information about the nature of interaction of 4-NP with adsorbent and to evaluate the applicability and efficiency of any adsorbent [26]. Fig. 8 shows adsorption isotherms at different temperature. The surface property can be determined as a multilayer or monolayer by using of adsorption isotherms. The Langmuir (8) and Freundlich (9) isotherm models are usually used to detect the adsorption isotherm.

$$C_e / q_e = 1 / b Q_{\max} + C_e / Q_{\max} \quad (8)$$

q_e (mgg^{-1}), C_e (mgL^{-1}), Q_{\max} (mgg^{-1}) and b (Lmg^{-1}) are the quantity of phenol adsorbed at equilibrium, the remaining concentration of phenol in solution at equilibrium, maximum adsorption capacity and Langmuir constant respectively which are relative to adsorption energy [27, 28]. The Langmuir model is monolayer adsorption isotherm. According to Langmuir isotherm, surface of adsorbent is homogeneous, energetically uniform [28]. Linear representation of Langmuir isotherm may be described by Eqn. (8). The Q_{\max} and b values were computed from the slopes and intercept of the linear plot of C_e/q_e versus C_e in Fig. 9 (A).

$$\log q_e = \log k + (1/n) \log C_e \quad (9)$$

k (mg/g) and n are the adsorbent capacity, the heterogeneous factor respectively and connected to intensity of Freundlich isotherm. According to Freundlich isotherm, adsorbent surface is heterogenous [29] and adsorption capacity is relative to the concentration of adsorbed

phenol at equilibrium. Freundlich isotherm is convenient adsorption at high concentrations and not convenient for low concentration range [30]. The values of k and n may be acquired from the slope and intercept of linear plot of $\log q_e$ versus $\log C_e$ [31]. In Fig. 9 (B) for based on Eqn. (9). The adsorption isotherm parameters, correlation coefficients (R^2) and values error RMSE (root mean squared error) were given in Table 2. The values of RMSE (Eqn.10) can be calculated by the following equations [21]:

$$RMSE = \sqrt{\frac{1}{n-1} \sum_{n=1}^n (q_{e,meas} - q_{e,cal})^2} \quad (10)$$

$q_{e,meas}$ (mg g^{-1}), $q_{e,cal}$ (mg g^{-1}) and n are the experimental, calculated equilibrium adsorption capacity and the value the number of data points respectively. According to Table 2, the Freundlich model provided a higher correlation coefficient ($R^2 = 0.7973, 0.8883$ and 0.8513) as compared to Langmuir isotherm model ($R^2 = 0.3780, 0.5450$ and 0.7290). It can be seen that the values of RMSE obtained from Freundlich were lower than those from the Langmuir. Low RMSE values indicate the accurate fitting of the model [21, 23]. According to the Freundlich isotherm, the significance of n value is as follows: adsorption process is chemical ($n < 1$), linear ($n = 1$), or physical ($n > 1$) [18]. From Table 2, the values of n are 1.2, 1.47 and 1.58 at 298, 313 and 328 K respectively. So, the adsorption of 4-NP on PVA/AC was a physical process due to $n > 1$.

Based on these results, the Freundlich isotherm model was the best-fitted adsorption isotherm model for the adsorption of 4-NP on PVA/AC. So, the adsorption of 4-NP on the PVA/AC occurred on nonhomogeneous adsorptive sites [31].

Table 2: Equilibrium parameters

T (K)	Langmuir isotherm				Freundlich isotherm			
	Q_{max} (mg g^{-1})	b (L mg^{-1})	R^2	RMSE	k (mg g^{-1})	n	R^2	RMSE
298	217.39	0.00214	0.3780	22	1.25	1.20	0.7973	18
313	238.10	0.00297	0.5450	16	2.32	1.47	0.8883	14
328	138.89	0.00536	0.7290	17	2.45	1.58	0.8513	13

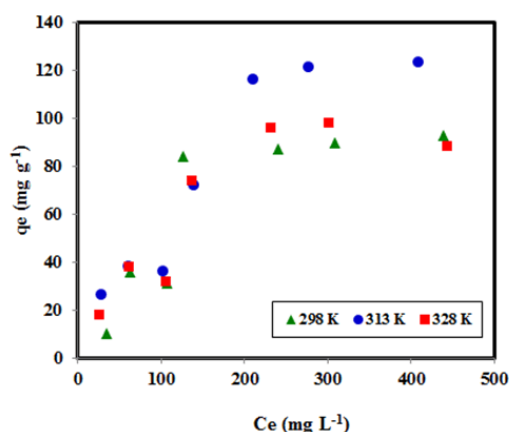


Figure 8: Adsorption isotherm of 4-NP on PVA/AC at different temperature

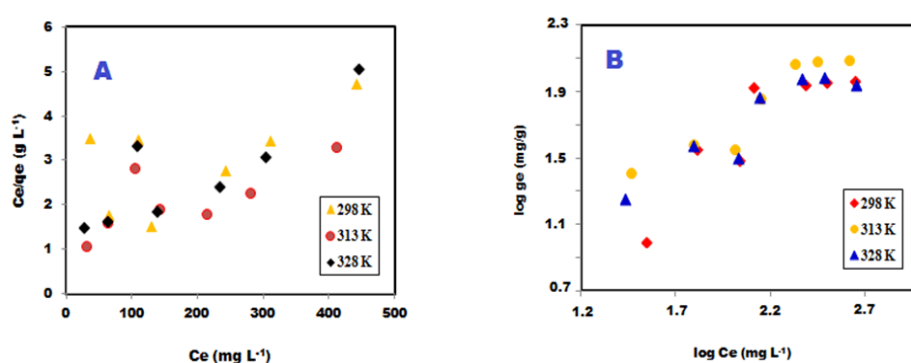


Figure 9: Langmuir (A) and Freundlich isotherm (B) plots for 4-NP removal by PVA/AC

3.9. Adsorption thermodynamics

The standard Gibbs energy change (ΔG°), standard enthalpy change (ΔH°) and standard entropy change (ΔS°) which are thermodynamic parameters. They are essential to predict the feasibility and mechanism of adsorption process. ΔG° was computed by using Eqn. (11). K_c (L/g) was calculated by using the Langmuir constants Q_{max} and b ($K_c = Q_{max} \times b$) (Fig. 10) and known as equilibrium constant [26]. R and T had been explained before.

$$K_c = Q_{max} \times b \quad (11)$$

The thermodynamic parameters ΔH° and ΔS° were computed by using the slope and intercept of the plot of $\ln K_c$ versus $1/T$, Fig. 10. The ΔG° was computed as 1.91, 0.91 and 0.82 kJ mol^{-1} at 298, 313 and 328 K respectively. Physical adsorption was reconfirmed because of ΔG° being $> -20 \text{ kJ mol}^{-1}$ regardless of the temperature, because these ΔG° values are positive. Therefore, this reaction is nonspontaneous. As the adsorption temperatures increased, accordingly the absolute values increased, which means the process becomes more non spontaneous at higher

temperatures [32]. According to Fig. 10, ΔS° and ΔH° were calculated as $37.32 \text{ J mol}^{-1} \text{ K}^{-1}$ and $12.88 \text{ kJ mol}^{-1}$ respectively. Owing to the positive ΔH° values, adsorption process is endothermic for 4-NP. Consequently, increasing the temperature from 298 to 328 K causes an increase in phenol adsorption on the PVA/AC. In addition, if the magnitude of ΔH if lies between 80–200 kJ/mol process of the adsorption may be considered as chemical whereas physical adsorption usually is seen in a range of 2.1–20.9 kJ/mol or $\leq 40 \text{ kJ/mol}$ [33]. In this way, adsorption of 4-NP on PVA/AC composite is physical in the nature (ΔH° were calculated as $12.88 \text{ kJ mol}^{-1}$). Positive ΔS° values show the increasing randomness in phenol solution-sorbent interface during the sorption process [27].

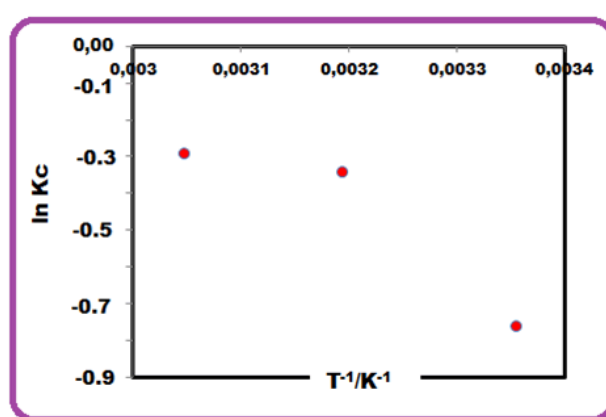


Figure 10: Van't Hoff plot of $\ln K_c$ versus $1/T$

4. Conclusion

In this study, PVA/AC composite was synthesized and characterized. The adsorption of 4-NP from aqueous solution was investigated by utilizing as an adsorbent PVA/AC. This adsorbent can be used for the elimination of 4-NP from aqueous solution. There were two kinds of the adsorption process parameters. They were kinetics and thermodynamic parameters and both of them were calculated. According to results, adsorption process was determined as endothermic. The adsorption isotherms were determined by Langmuir and Freundlich models. The adsorption data was better fitted by the Freundlich isotherm model due to RMSE and R^2 values. Adsorption kinetic model was determined as a pseudo-first-order kinetic model. All the results on the sorption of 4-NP on PVA/AC indicate the applicability of the adsorption study.

Acknowledgement

This research was supported by the Scientific Research Project of Dicle University (Project Number: Fen.18.008).

References

- [1] Aljeboree, A., Alshirifi, A., Alkaim, A., *Kinetics and equilibrium study for the adsorption of textile dyes on coconut shell activated carbon*, *Arabian Journal of Chemistry*, 10, 3381-3393, 2017.
- [2] Wang, H., *Preparation and properties of porous poly (vinyl alcohol)/powdered activated carbon composite*, *Material Science and Advanced Technologies in Manufacturing*, 852, 117-120, 2014.
- [3] Jia, Z., Li, Z., Li, S., Li, Y., Zhu, R., *Adsorption performance and mechanism of methylene blue on chemically activated carbon spheres derived from hydrothermally-prepared poly (vinyl alcohol) microspheres*, *Journal of Molecular Liquids*, 220, 56–62, 2016.
- [4] Kaur, T., Thirugnanam, A., *Effect of Porous Activated Charcoal Reinforcement on Mechanical and In-Vitro Biological Properties of Polyvinyl Alcohol Composite Scaffolds*, *Journal of Materials Science & Technology*, 33(7), 734–743, 2017.
- [5] Kumar, A., Kumar, S., Kumar, S., Gupta, D., *Adsorption of phenol and 4-nitrophenol on granular activated carbon in basal salt medium: equilibrium and kinetics*, *J. Hazard. Mater.*, 147, 155–166, 2007.
- [6] Liu, S., Wang, J., Huang, W., Tan, X., Dong, H., Goodman, B., Du, H., Lei, F., Diao, K., *Adsorption of phenolic compounds from water by a novel ethylenediamine rosin-based resin: Interaction models and adsorption mechanisms*, *Chemosphere*, 214, 821-829, 2019.
- [7] Ivanov, A., Kozynchenko, O., Mikhalovska, L., Tennison, S., Jungvid, H., Gunko, V., Mikhalovsky, S., *Activated carbons and carbon-containing poly(vinyl alcohol) cryogels: characterization, protein adsorption and possibility of myoglobin clearance*, *Phys. Chem. Chem. Phys.*, 14, 16267–16278, 2012.
- [8] Swamy, M., Nagabhushana, B., Krishna, R., Kottam, N., Raveendra, R., Prashanth, P., *Fast adsorptive removal of methylene blue dye from aqueous solution onto a wild carrot flower activated carbon: isotherms and kinetics studies*, *Desalination and Water Treatment*, 71, 399–405, 2017.
- [9] Silva, M., Santos, M., Júnior, M., Fonseca, M., Filho, E., *Natural Palygorskite as an Industrial Dye Remover in Single and Binary Systems*, *Materials Research*, 19, 1232-1240, 2016.
- [10] Trivedi, M., Sethi, K., Panda, P., and Jana, S., *A comprehensive physicochemical, thermal, and spectroscopic characterization of zinc (II) chloride using X-ray diffraction, particle size distribution, differential scanning calorimetry, thermogravimetric analysis/differential thermogravimetric analysis, ultraviolet-visible, and Fourier transform-infrared spectroscopy*, *International Journal of Pharmaceutical Investigation*, 7, 33-40, 2017.
- [11] Cuevas, L., Villacura, E., Toloza, C., *Magellan Peat (Sphagnum Magallanicum) As Natural Adsorbent Of Recalcitrant Synthetic Dyes*, *J. Soil Sc. Plant Nutr.*, 8, 31-43, 2008.
- [12] Haddad, M., Mamouni, R., Saffaj, N., Lazar, S., *Removal of a cationic dye – Basic Red 12– from aqueous solution by adsorption onto animal bone meal*, *Journal of the Association of Arab Universities for Basic and Applied Sciences*, 12, 48–54, 2012.
- [13] Dhorabe, P., Lataye, D., Ingole, R., *Removal of 4-nitrophenol from aqueous solution by adsorption onto activated carbon prepared from Acacia glauca sawdust*, *Water Science & Technology*, 73, 2016, doi: 10.2166/wst.2015.575.
- [14] Chartarrayawadee, W., Moulton, S., Too, C., Wallace, G., *Fabrication of Graphene Electrodes by Electrophoretic Deposition and Their Synergistic Effects with PEDOT and Platinum*, *Chiang Mai J. Sci.*, 40, 750-762, 2013.

- [15] El-Naggar, N., Hussein, M., El-Sawah, A., *Phycobiliprotein-mediated synthesis of biogenic silver nanoparticles, characterization, in vitro and in vivo assessment of anticancer activities*, *Scientific Reports*, 8, 2018, doi:10.1038/s41598-018-27276-61.
- [16] Paralikar, P., *Biogenic Synthesis of Silver Nanoparticles Using Leaves Extract of Epiphyllum Oxypetalum and its Antibacterial Activity*, *Austin Journal of Biotechnology & Bioengineering*, 1, 2014.
- [17] Bulut, Y., Karaer, H., *Adsorption of Methylene Blue from Aqueous Solution by Crosslinked Chitosan/Bentonite Composite*, *Journal of Dispersion Science and Technology*, 36,61-67, 2015.
- [18] Salehi, E., Farahani, A., *Macroporous chitosan/polyvinyl alcohol composite adsorbents based on activated carbon substrate*, *J Porous Mater.*, 24,1197–1207, 2017.
- [19] Feyzi, F., Jalilvand, H., Dehghani, M., *Adsorption of dimethyl sulfide from model fuel on raw and modified activated carbon from walnut and pistachio shell origins:kinetic and thermodynamic study*, doi.org/10.1016/j.colsurfa.2020.124620.
- [20] Nam, H., Nam, H., Wang, S., *Preparation of activated carbon from peanut shell with KOH activation and its application for H₂S adsorption in confined space*, *Journal of Environmental Chemical Engineering*, 8, 103683, 2020.
- [21] Fajri, L., Nawi, M., Sabar, S., Nawawi, N., *Preparation of immobilized activated carbon-polyvinyl alcohol composite for the adsorptive removal of 2,4-dichlorophenoxyacetic acid*, *Journal of Water Process Engineering*, 25, 269–277, 2018.
- [22] Almeida, V., Vargas, A., Nogami, E., *NaOH-activated carbon of high surface area produced from coconut shell: Kinetics and equilibrium studies from the methylene blue adsorption*, *Chemical Engineering Journal* 174, 117– 125, 2011.
- [23] Tseng, T., Wu, F., Juang, R., *Characteristics and applications of the Lagergren's first-order equation for adsorption kinetics*, *Journal of the Taiwan Institute of Chemical Engineers* 41, 661–669, 2010.
- [24] Wang, L., Zhang, J., Wang, A., *Fast removal of methylene blue from aqueous solution by adsorption onto chitosan-g-poly(acrylic acid)=attapulgitic composite*. *Desalination*, 266: 33–39, 2011.
- [25] Gürses, A., Hassani, A., Kirans, M., Açışlı, O., Karaca, S., *Removal of methylene blue from aqueous solution using by untreated lignite as potential low-cost adsorbent: kinetic, thermodynamic and equilibrium approach*, *J. Water Process Eng.*, 2,10-21, 2014.
- [26] Daga, K., Gehlot, P., *Use of Polyvinylalcohol Coated Carbon Black for Removal of Linear AlkylbenzeneSulphonate (Las) From Wastewater*, *Nature Environment and Pollution Technology* © Technoscience Publications, 6,725-730, 2007.
- [27] Karaer, H., Kaya, I., *Synthesis, characterization of magnetic chitosan/active charcoal composite and using at the adsorption of methylene blue and reactive blue4*, *Microporous and Mesoporous Materials*, 232,26-38, 2016.
- [28] Iqbal, M., Ashiq, M., *Adsorption of dyes from aqueous solutions on activated charcoa*, *Journal of Hazardous Materials B*, 139,57–66, 2007.
- [29] Karaer, H., Uzun, İ., *Adsorption of basic dyestuffs from aqueous solution by modified chitosan*, *Desalination and Water Treatment*, 51, 2294-2305, 2013.
- [30] Negma, N., AbdElWahed, M., Hassan, A., Kana, M., *Feasibility of metal adsorption using brown algae and fungi: Effect of biosorbents structure on adsorption isotherm and kinetics*, *Journal of Molecular Liquids*, 264, 292–305, 2018.

[31] Kyzas, G., Deliyanni, E., Lazaridis, N., *Magnetic modification of microporous carbon for dye adsorption*, *Journal of Colloid and Interface Science*, 430,166–173, 2014.

[32] Kim, Y., Kim, J., *Isotherm, kinetic and thermodynamic studies on the adsorption of paclitaxel onto Sylopute*, *J. Chem. Thermodynamics*, 130,104–113, 2019.

[33] Mahida, V., Patel, M., *Removal of some most hazardous cationic dyes using novel poly(NIPAAm/AA/N-allylisatin) nanohydrogel*, *Arabian J. Chem.*, 9, 430-442, 2016.